The Journal of Neuroscience, December 1989, 9(12): 4253–4268

Task-Dependent Field Potentials in Human Hippocampal Formation

Gregory McCarthy, Charles C. Wood, Peter D. Williamson, and Dennis D. Spencer

Neuropsychology Laboratory, Veterans Administration Medical Center, West Haven, Connecticut 06516, and Section of Neurosurgery and Department of Neurology, Yale University School of Medicine, New Haven, Connecticut 06520

Task-dependent field potentials were recorded from implanted electrodes located in the hippocampus and other medial temporal lobe (MTL) structures of epileptic patients undergoing evaluation for possible surgery. In 2-alternative categorization tasks, low-probability auditory, somatic, and visual stimuli elicited potentials with large amplitudes and sharp spatial gradients having the following characteristic spatial distribution: positive posterior to the hippocampus, negative within the hippocampus, and positive anterior to the hippocampus. The sharp spatial gradients within the MTL suggest that these potentials were locally generated, probably by hippocampal pyramidal cells. The MTL potentials were also reliably elicited by exemplars of semantic categories and by stimulus omissions and were sensitive to the sequence of preceding stimuli. However, they were not elicited by the same stimulus sequences when the patient's attention was directed elsewhere and categorization was not required. These results indicate that the MTL potentials reflect endogenous as opposed to obligatory processes. The time course and task dependence of the MTL potentials suggest that MTL structures could contribute to P300 and related event-related potentials on the scalp.

In this paper we describe task-dependent field potentials recorded from electrodes located in the medial temporal lobe (MTL) in and near the hippocampal formation and amygdala in humans undergoing evaluation for neurosurgical treatment of intractable epilepsy (Williamson et al., 1980; Spencer et al., 1982). Task-dependent potentials are a class of event-related potentials (ERPs) sensitive to the context in which the eliciting stimuli are presented and relatively insensitive to their physical characteristics. The tasks employed are those that have been used previously to elicit P300, an ERP first described in scalp recordings by Sutton (Sutton et al., 1965, 1967) and thought to reflect neural activity associated with cognitive processes. We seek to identify neural structures that could contribute to P300 and, by inference, the psychological processes reflected by its occurrence.

The search for the neural generators of P300 is given strong impetus by the psychological processes with which it has been associated. P300 is most reliably elicited by stimuli that are *a priori* uncertain and that either signal a choice or provide task-relevant feedback. In simple discrimination or categorization tasks, P300's amplitude is dependent upon the sequence of preceding stimuli, indicating that subjects' expectancies are important determining factors (Squires et al., 1976a). The latency of P300 is positively correlated with the time required to identify the category membership of the stimulus (Kutas et al., 1977; McCarthy and Donchin, 1981, 1983), indicating that the processes associated with P300 are subsequent to and contingent upon the stimulus identification. That P300 is associated with processes concerned with abstract or representations of the stimulus is suggested by the fact that it can be elicited by stimuli of any modality and by the omission of a stimulus if the omission constitutes a task relevant event (Sutton et al., 1967).

A generally accepted theoretical account of P300 in psychological terms is still lacking (Donchin and Coles, 1988; Verleger, 1988). An influential model was advanced by Donchin (1981), who postulated that P300 reflects the operation of processes associated with the revision of schema guiding the subject's expectancies for future events. This association of P300 with the modification of memory is also a prominent feature in the model of Halgren et al. (1983). Alternative hypotheses have been proposed by Desmedt (1980) and Verleger (1988).

Regardless of the specific psychological processes associated with P300, it has found increasing use as a tool in studies of development (Courchesne et al., 1987), aging (Goodin et al., 1978; Pfefferbaum et al., 1984), dementia (Goodin et al., 1983; Polich et al., 1986), schizophrenia (Roth et al., 1980), alcoholism (Polich, 1984), and epilepsy (McCarthy et al., 1987; Meador et al., 1987; Wood et al., 1988). This clinical use of P300 thus provides an independent incentive for an explication of its neural generators.

In scalp recordings, P300 is usually identified as a positivity (relative to ear, mastoid, or nose reference) with a maximum amplitude over the midline parietal scalp, a peak latency typically within the range of 300–600 msec, and a duration often greater than 300 msec. Changes in the shape of the scalp voltage distribution over the duration of P300 indicate that multiple neural generators with overlapping time courses are active. The ambiguity of scalp recordings with respect to the number and configuration of neural generators has been a major limitation in the interpretation of ERPs (Allison et al., 1986). In some tasks, the waveform comprising P300 has been fractionated into a complex of temporally overlapping components including N200 (Simson et al., 1977), an anterior P3a and posterior P3b (Squires et al., 1975), and one or more long-duration negative and positive slow waves (Squires et al., 1976b; Rohrbaugh et al., 1978; Ruchkin et al., 1980). Further fractionation has been proposed by some (Friedman et al., 1981), who use the term late positive

Received Jan. 30, 1989; revised May 30, 1989; accepted June 5, 1989.

We thank Mary Pearson for help in preparing the figures, Dennis Thompson, Joseph Jasiorkowski, and Elizabeth Roessler for technical assistance, Dr. Terrance Darcey for the estimates of electrode positions, and Drs. Truett Allison, Kenneth Paller, and Marta Kutas for helpful comments. Supported by the Veterans Administration and NIMH Grant MH-05286

Correspondence should be addressed to Gregory McCarthy at the above address.

 0270-6474/89/124253-16$02.00/0

complex to refer to the aggregate. A complete specification of the neural generators of P300 will depend upon models which account for all of the spatial and temporal features of the scalp potential field.

In the present studies, a 2-alternative categorization (or *oddball*) task widely used to investigate scalp P300 was used to investigate its intracranial concomitants. In such a task, 2 stimulus categories are presented in random sequence with asymmetric probabilities (e.g., 0.8/0.2 or 0.9/0.1). Prominent P300s are elicited by the low-probability (target) stimuli when subjects are required to respond overtly or covertly (e.g., by keeping a mental count) to them. Similar tasks were used by Halgren et al. (1980, 1986), Stapleton and Halgren (1987), and Wood et al. (1980) in prior investigations of P300-like ERPs in the MTL, and by others in studies of thalamus (Yingling and Hosobuchi, 1984), cortex, and other regions (Curry and McCallum, in Wood et al., 1984). Animal models for P300 have also employed variants of this task in rabbits (Gabriel et al., 1983), cats (Buchwald and Squires, 1981; Wilder et al., 1981), monkeys (Arthur and Starr, 1984; Neville and Foote, 1984; Paller et al., 1988), and dolphins (Woods et al., 1985). The data presented here were obtained from tasks using auditory, somatic, and visual stimuli, as well as stimulus omissions. Categories were defined by simple physical characteristics or by semantic rules.

Materials and Methods

Patients. Recordings were made in a group of 90 patients (50 male) with complex partial epilepsy of diverse etiologies studied with multicontact depth electrodes between August 1980 and May 1988. Each patient had debilitating seizures inadequately controlled by anticonvulsant medications, and all were participants in a comprehensive evaluation program which included implantation of depth probes to localize the epileptogenic focus (Williamson et al., 1980). Probes remained in place for 5–15 d, during which time the patient's intracranial EEG was continuously monitored to determine the locations of seizure foci. ERP recordings were obtained concurrently with EEG monitoring, usually on the third and fourth day following implantation. The ERP recordings were approved by the Human Investigations Committees of Yale University and the West Haven VA Medical Center, and informed consent was obtained. The patients ranged in age from 16 to 47 (mean = 29.7). Full scale WAIS IQ averaged 92 (SD = 13.5 range of 70–134).

Depth probes. Each depth probe was constructed of 18 platinum-iridium wires (0.0035 inch diameter) surrounding a core composed of 24-gauge stainless steel needle stock. The recording contacts were exposed, platinized 1 mm sections of wire equally spaced along each probe from point of insertion (contact 1 in all figures) to the distal tip (contact 18). Typical electrode impedances were 10–40 kΩ. The low-frequency response of each contact was approximately 0.06 Hz (−3 dB).

The probes were inserted through stereotaxically placed stainless steel guide pins. Within the constraints of differing cerebral vasculature, each probe followed 1 of 5 standard trajectories referred to as frontal, supplemental, posterior cingulate, midtemporal, and posterior–temporal. This report concerns recordings made from left and right posterior–temporal (LP and RP) and left and right midtemporal probes (LM and RM). The LP and RP probes entered the brain near the parieto-occipital border and were intended to penetrate the hippocampus over much of its length, terminating in or beyond the amygdala. The RM and LM probes entered the frontal lobe and passed into the anterior temporal lobe in the region of the amygdala. The mid- and posterior–temporal probes crossed near their distal tips in the vicinity of the anterior hippocampus and amygdala. Different probe lengths with differing interelectrode spacings were used to accommodate the variation in brain size. The modal interelectrode spacings were 5.0 mm (range, 4.6–5.6 mm) for the midtemporal probes and 6.1 mm (3.3–6.1 mm) for the posterior–temporal probes.

The number of probes and their placement were determined solely on clinical grounds. From 1–8 probes were implanted in each patient, typically 3–4. Sixty-seven patients had bilateral and 21 had unilateral posterior–temporal probes (14 LP and 7 RP). Fifty-one patients had bilateral and 3 had unilateral midtemporal probes (2 LM and 1 RM). In addition to implanted probes, some patients had scalp or epidural recording pins and 33 had subdural multielectrode strips. These strips contained 7 or 8 recording contacts spaced at 1 cm intervals and were usually placed unilaterally over the lateral surface of the temporal lobe. Comprehensive scalp distributions of P300 using a 50 electrode scalp montage were obtained in most patients several days prior to implant surgery (McCarthy et al., 1987).

Electrode localization. The location of recording contacts with respect to brain structures was estimated using a computerized method (Darcey and Williamson, 1985) based on the atlas of Talairach and Szikla (1967). The procedure involved digitizing lateral and frontal X-rays taken of the head with implanted guide pins during surgery while the patient was in the stereotaxic apparatus. The positions of the external auditory meatus, the bony sulcus of the transverse sinus, and the tuberculum sellae were used to project the position of each contact into the standardized coordinate system of the atlas, allowing comparison to sections from sample brains. Drawings of probe contacts superimposed upon schematic drawings from Talairach and Szikla (1967) appear frequently throughout this paper to provide estimates for electrode location. The estimation error in this procedure is difficult to determine, but errors of 3–5 mm are possible, making it difficult to determine whether contacts near the border of a structure are inside or out. Relatively few standardized frontal views are provided in the atlas so that the medial–lateral position of only those contacts at those section levels could be represented.

Recording parameters. Up to 64 recording contacts were simultaneously amplified and digitized. In some cases, the number of contacts sampled was increased by repeating tasks with alternate montages. All recordings were made to a common reference, which was either an EKG-balanced sternovertebral pair, linked ears, or a single ear. Essentially equivalent recordings were obtained with each reference due to the much larger amplitudes of the intracranial potentials relative to surface recordings. All signals were electrically isolated and amplified through a bandpass of 0.1–100 Hz (−3 dB). The EEG from each contact was digitized at 4 or 5 msec/point for a 1 sec epoch beginning 100 msec prior to stimulus presentation. In some cases a sampling rate of 6 msec/point was used. The single trial epochs were averaged on-line according to stimulus category and, in some cases, were saved individually for off-line analyses.

Field potential analysis. Because the number and exact placement of depth probes differed from patient to patient, it was not possible to analyze these data using conventional across-subject statistical procedures. We will therefore illustrate the consistent features of the data and their variability in 3 ways: (1) by detailed intracranial potential distributions under the same conditions for a number of individual patients; (2) by measures of central tendency and variability of peak amplitudes and latencies across patients; and (3) by spatial plots of peak amplitudes across patients.

Current source density (CSD) analysis, which allows the locations and time courses of current sources and sinks to be estimated from extracellular field potential recordings, is one of the strongest types of evidence concerning generator localization (Nicholson and Freeman, 1975; Wood and Allison, 1981; Mitzdorf, 1985). Unfortunately, the assumptions required for CSD, even in its restricted 1-dimensional form, are not justified given the clinical constraints of our recordings. One-dimensional CSD requires recordings at high spatial resolution (50–100 μm) along a major anatomical axis of the tissue in question, homogeneity of conductivity along that axis, and absence of significant potential gradients along the 2 perpendicular axes. None of these assumptions is adequately met by our recordings, which were obtained at 3–6 mm intervals over 7–14 mm trajectories that penetrated cortex, white matter, ventricles, multiple regions of the hippocampus, and amygdala. However, while the data do not justify formal CSD computation, their spatial extent and resolution are sufficient to allow regions of maximal spatial gradient of potential to be identified as probable field potential generators. Large spatial gradients of potential will therefore receive major emphasis in Results.

Categorization tasks. The tasks used with all patients involved the presentation of runs of 200 stimuli composed of 2 categories. Order of presentation was random with the probability of occurrence of a stimulus from one category being 80% (the *standards*), while the other was 20% (the *targets*). The interval between successive stimuli within a run was fixed at 1200 msec. In COUNT tasks, patients were required to count mentally the number of targets presented and report that count at the

end of the run. The patients were admonished from subvocalizing or using their fingers to maintain the count. In IGNORE tasks, identical runs of stimuli were presented, but the patient was instructed not to count targets and was given instead a magazine to read.

Auditory, somatic, and visual stimuli were used in different conditions. Auditory standards were 500 μsec clicks delivered through earphones at 60 dB SL, while targets were 10 μsec clicks which sounded much softer. In some patients, 1000 and 1200 Hz tone pips were used as standards and targets. Somatic standards were 500 μsec shocks delivered to the right or left median nerve at the wrist from an isolated constant-current stimulator. The stimulus intensity (1.5–3.0 mA) was adjusted so that a twitch of the right thumb was just detectable. Targets were 100 μsec shocks delivered at the same intensity to the same nerve but which were perceptually less intense. For some patients, both targets and standards were presented at twitch threshold with standards delivered to one wrist and targets delivered to the opposite wrist.

There were 2 visual conditions, one requiring a discrimination based upon the physical appearance of the stimuli and the other depending upon a semantic judgment. In the visual x/o condition, standards were a string of xxxxx characters and targets a string of ooooo characters presented on a CRT. In the NAMES condition, common and unambiguous female and male names were used, respectively, as standards and targets. All names were either 4 or 5 characters long, and while the probabilities of occurrence of standards and targets were 0.80/0.20 as before, the number of exemplars from each category was adjusted so that each individual name was presented with the same probability. In both visual conditions the character strings were exposed for 200 msec.

In addition to COUNT and IGNORE, an OMIT task was used in which targets were omissions from a train of standard auditory clicks. Omissions occurred on 10% of the trials constrained so that 2 omissions did not occur in immediate sequence.

The number of tasks and replications varied as clinical considerations determined the time available for testing. In the auditory modality, COUNT was run with 85 patients, OMIT with 14, and IGNORE with 17. Somatic tasks were run with 17 patients, visual x/o with 41, and NAMES with 36.

Results

Intracranial and scalp recordings of ERPs obtained simultaneously from patient B10 in the auditory COUNT task are presented in Figure 1. P300 can be observed as a slow positive potential at the midline posterior (P_z) scalp beginning at the termination of the negative potential at 230 msec (N200) and persisting until 800 msec. The intracranial ERPs, obtained from 3 consecutive contacts near the posterior hippocampus (LP 7–9) and a more anterior contact (LP 13), illustrate the essential components of a pattern characteristic of our sample. Targets elicited a broad positive potential (70 μV) with a peak latency of about 400 msec posterior to the hippocampus at LP 8 with smaller positivities at LP 7 and other more posterior sites. A negative ERP roughly similar in onset and duration but much larger in amplitude (−198 μV at 412 msec) was obtained more anteriorly at LP 9. The large negativity diminished in amplitude at more anterior probe positions until LP 13, where a positive ERP was again recorded. The large positive ERPs at LP 8 and LP 13 were preceded by sharp negative potentials of similar latency to scalp N200, while the large negative potential at LP 9 was preceded by a smaller positive potential. The scalp and intracranial ERPs had similar onset latencies and durations, but waveshape differences were also apparent.

A more extensive distribution of MTL ERPs elicited in the auditory COUNT task is presented for patient A7 in Figure 2. P300 can be seen in the target scalp ERPs obtained a few days prior to implant surgery using identical stimuli. As is typically observed, P300 was broader and later in peak latency at the posterior (P_z) as compared with frontal (F_z) scalp sites.

A target ERP similar to that obtained at the posterior scalp can be seen at RP 9 near the posterior margin of the hippocampus, although its peak amplitude (41 μV) is 5 times greater than the scalp P300. As in Figure 1, this positive ERP was preceded by a sharp negative ERP at about 250 msec. Smaller-amplitude positive potentials were obtained from more posterior contacts along the probe, including RP 1, which is redrawn below the scalp ERPs at the equivalent scale. At RP 10, a large negative ERP is elicited by the target, similar in onset and peak latency to the positive ERP at RP 9, but larger in peak amplitude (−103 μV). Similar negative potentials of smaller amplitude were obtained at contacts RP 11–13. At RP 14, superior to the anterior hippocampus, and at RP 15, estimated to be within the amygdala, the target ERPs were again marked by positive potentials. Similar positive potentials were obtained along the remainder of the probe.

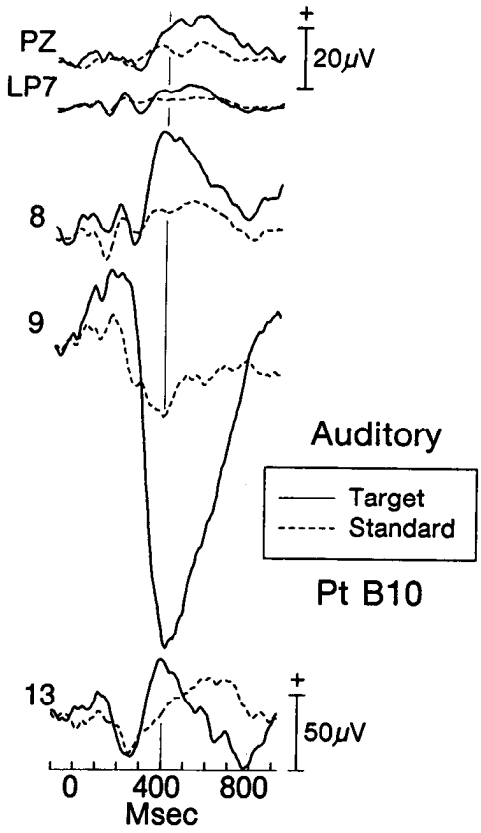

Figure 1. Scalp and intracranial ERPs simultaneously obtained during the auditory COUNT task in patient B10. Note the different voltage calibration for scalp and intracranial ERPs. In this and subsequent figures, an isolatency line at 400 msec is drawn to facilitate waveform comparisons.

The RM probe passed through the anterior hippocampus. At RM 9, located in frontal lobe white matter, no large differences were apparent between target and standard ERPs. At RM 15, just superior to the hippocampus, the target ERP was marked by a positive potential similar to that described for RP 15. Within the hippocampus at RM 16, a negative potential similar in shape to those obtained from RP 10–13 was recorded. Thus, negative potentials were elicited by targets at locations judged to be in or very near the hippocampus, while positive potentials of approximately the same duration and waveshape were obtained at locations anterior and posterior to the hippocampus, as well as superior to the anterior hippocampus. Changes in

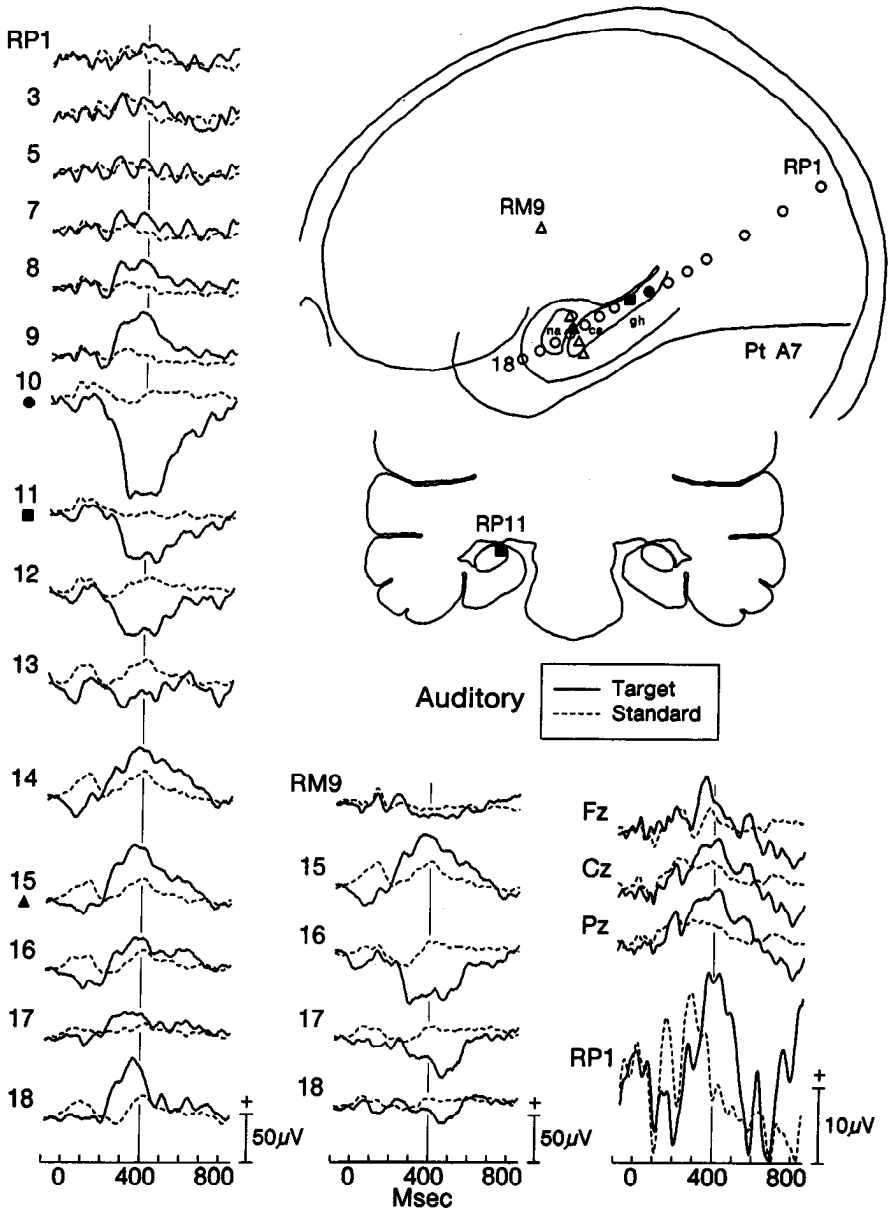

Figure 2. ERPs from patient A7 elicited by auditory COUNT target (*solid*) and standard (*dashed*) clicks from the right posterior (*left column*) and right medial temporal (*middle column*) probes, and from frontal (F_z), central (C_z), and posterior (P_z) midline scalp locations recorded 5 d prior to implant surgery (*right column*). The ERPs from RP1 are redrawn in the right column at the same amplitude calibration as the scalp recordings. The estimated locations of each RP contact for which ERPs are shown are depicted as *circles* on a sagittal view of the brain. The locations of RM contacts are depicted as *triangles*. RP 10–11 and RM 16 are depicted as *filled symbols*. The outlines of the hippocampus (*ca*), parahippocampal gyrus (*gh*), and amygdala (*na*) are taken from Talairach and Szikla (1967) using methods detailed in the text.

polarity occurred between locations near the estimated margins of the hippocampus.

The large ERP amplitudes and sharp spatial gradients (including polarity inversions between adjacent contacts) suggested that these potentials were generated within the MTL and not in distant tissue. This distributional pattern of P300-like ERPs will be referred to hereafter as the MTL pattern.

Task dependence

The occurrence of P300 in scalp recordings is dependent upon the experimental task and is not reliably evoked by a low-probability stimulus if it is not relevant to the subject's task (Squires et al., 1976b). We have found the MTL ERP pattern to be likewise task dependent as illustrated in Figure 3, where ERPs for identical low-probability stimuli from the auditory COUNT and IGNORE tasks are superimposed. In the COUNT task, a robust MTL pattern was elicited. However in a subsequent IGNORE task, the MTL ERP pattern was abolished. Task irrelevant clicks elicited little reliable MTL activity. The absence of the MTL ERPs to task irrelevant stimuli was consistent among our patients and is further illustrated in Figure 4.

The MTL pattern illustrated for counted targets in Figure 3 was similar to that shown in Figure 2 with the exception of an interposed flat ERP between the positive ERP recorded at LP 10 and the negative ERP recorded at LP 12. This transitional waveform at LP 11 occurred near the point where the probe appears to enter the hippocampus posteriorly.

Despite overall similarity, the target ERPs from intracranial locations in Figure 3 demonstrated more waveshape variability at adjacent contacts than those shown in Figure 2. The large negative ERPs at LP 15 and LP 14 had somewhat earlier onsets than those obtained at LP 12–13. The positive ERP at LP 10 was more similar in waveshape and time course to the negative ERP at LP 15 than to those at intervening contacts. Small differences in waveshapes were common among the MTL target ERPs, even at closely spaced contacts. These differences may

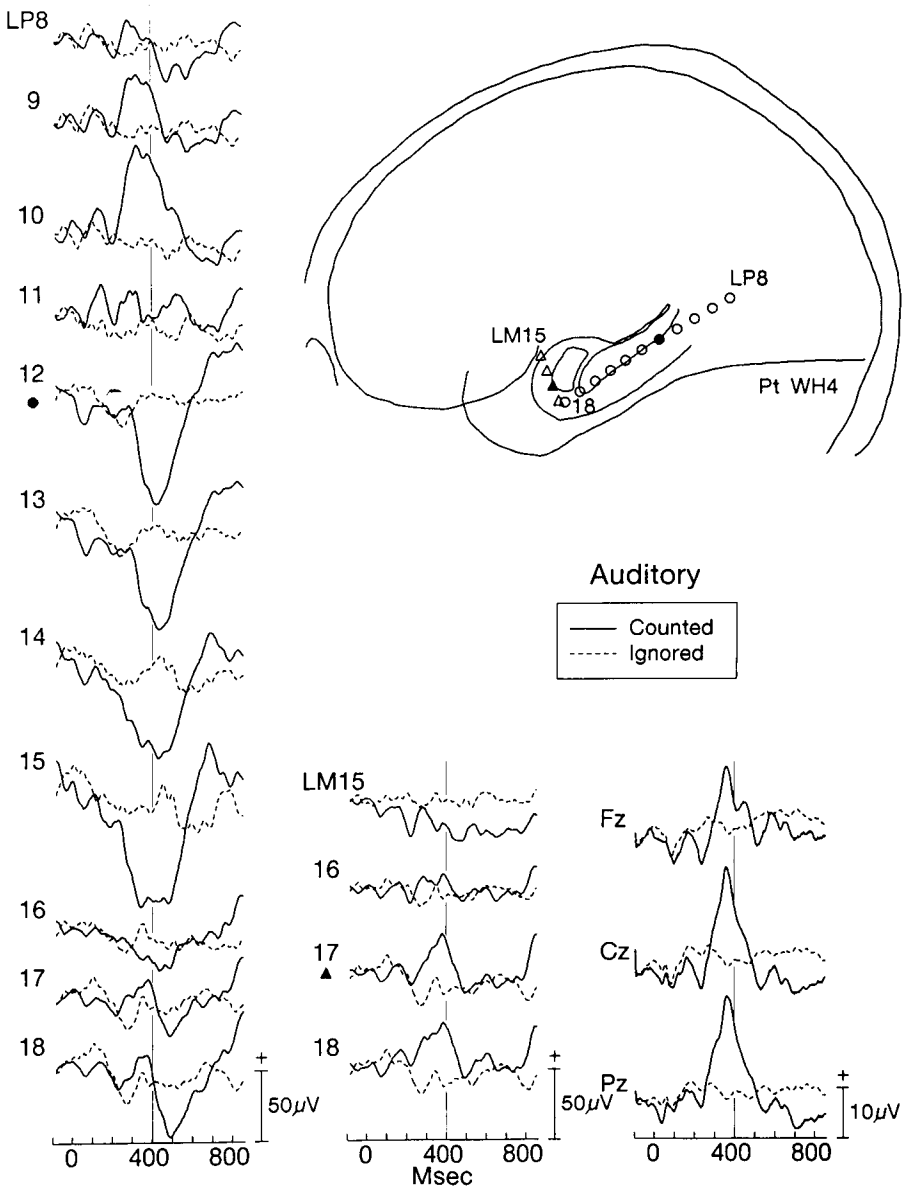

Figure 3. ERPs elicited by auditory COUNT (*solid*) and IGNORE (*dashed*) targets for LP (*circle*) and LM (*triangle*) contacts in patient WH4. LP 12 and LM 17 are depicted as *filled symbols*. Scalp-recorded ERPs elicited by auditory COUNT targets (*solid*) and standards (*dashed*) prior to implant surgery are shown in the rightmost column for comparison.

be due to the spatial arrangement of active neurons with respect to the electrodes and to differences in the timing of activation within the MTL.

The MTL pattern in Figure 4 was similar to that described previously with a transition from positive to negative ERPs occurring near the posterior margin of the hippocampus. The peak latency and waveshape of the negative ERP at LP 10 was the same as that of the P300 recorded from the posterior scalp prior to implant surgery. The positive ERPs obtained posterior to the hippocampus (LP 7–9) had 2 maxima, the first of which occurred earlier than the large negative peak at LP 10. Such a fractionation of these positive potentials was seen in several other patients. Unlike other patients, however, the anterior MTL target ERPs had only small broad positivities. Patient T10 later had a hamartoma removed from the left amygdalar region, which might account for this altered pattern of activity in the anterior MTL. We (Wood et al., 1984; McCarthy et al., 1987) and others (Squires et al., 1983; Meador et al., 1987) have noted that MTL potentials are often abnormal or absent in the temporal lobe in which the epileptogenic focus is found. Differences in the MTL pattern possibly due to pathological processes will be considered further below.

The data presented in Figures 1–4 illustrate the MTL pattern for auditory targets and the variation typical of our patient sample. Target ERPs from contacts which were both posterior and superior to the hippocampus had late positive potentials grossly similar to P300s recorded from scalp electrodes. While these positive potentials were often seen at the most superficial probe contacts (as shown in Fig. 2), they usually increased in amplitude as the probe approached the hippocampus. The transition to negative potentials of similar latency and larger amplitude occurred near the posterior margin of the hippocampus. In most patients, this inversion occurred between consecutive probe contacts, although a flat transitional waveform was sometimes interposed (as in Fig. 3, LP 11). The negative potentials often decreased in amplitude at more anterior locations within the hippocampus. Positive potentials were seen in the region of the amygdala with the transition usually occurring after the

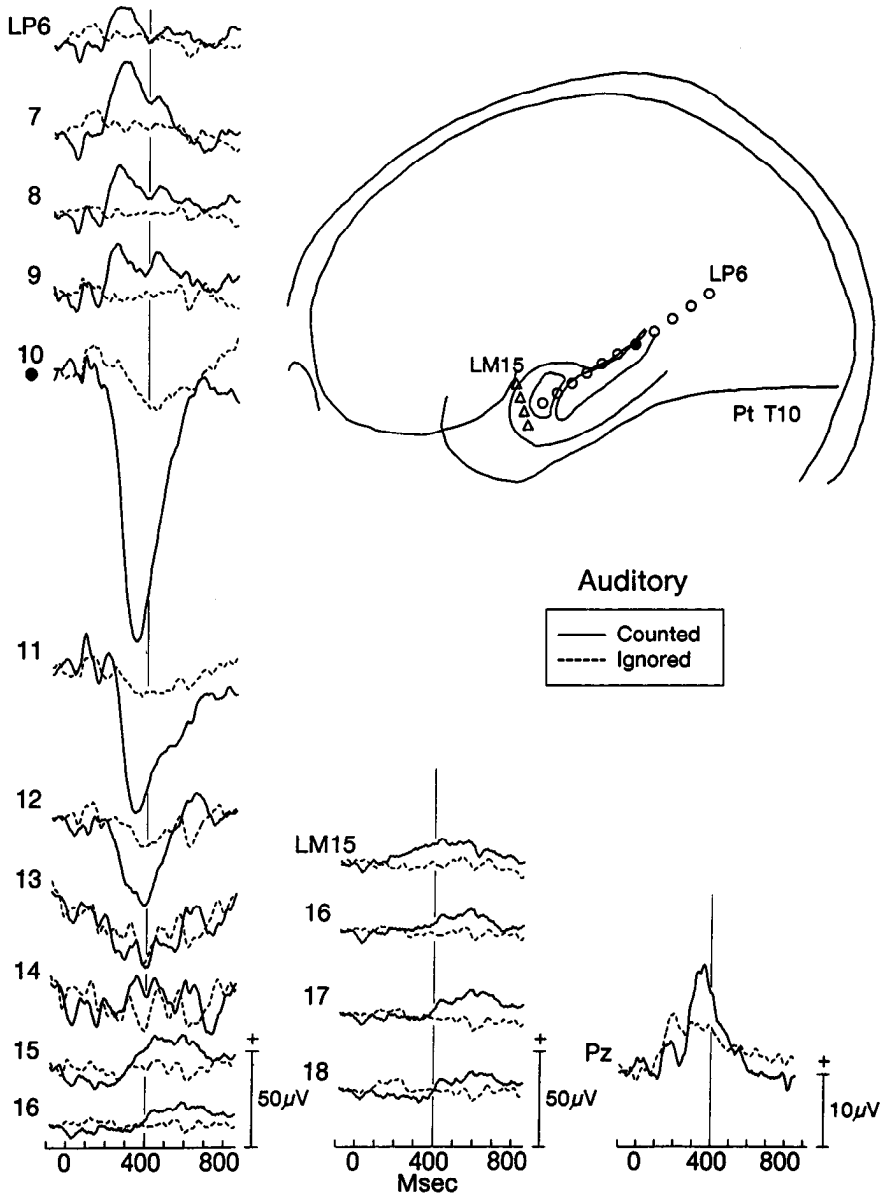

Figure 4. ERPs elicited by auditory COUNT (*solid*) and IGNORE (*dashed*) targets are shown for LP (*circle*) and LM (*triangle*) contacts in patient T10. LP 10 is depicted as a *filled circle.* Scalp ERPs elicited by auditory targets (*solid*) and standards (*dashed*) prior to implant are shown in the rightmost column for comparison.

probe exited the anterior hippocampus. ERPs elicited by standards and by ignored targets elicited little MTL activity.

The waveshapes of the potentials varied across patients. In some, such as in Figures 1 and 2, the waveshapes were similar and the latencies of the potential peaks were nearly the same. In Figure 3, the potentials comprising the MTL pattern overlapped but had different peak latencies and waveshapes. This was true even among the large negative potentials from nearby contacts within the hippocampal region. The data from patient T10 in Figure 4 presented a more extreme example of waveshape variability as the posterior positivities had 2 peaks.

Modality independence

Like scalp-recorded P300, the MTL pattern can be elicited by stimuli of any modality. Figure 5 presents recordings from patient B8 from the somatic COUNT task. Positivities were elicited by somatic targets at contacts posterior and dorsal to the hippocampus (RP 6–9). A negative potential was recorded at RP 11 and RP 14 and flat, transitional ERPs were recorded between at RP 12–13. Examination of the estimated probe trajectory suggested that these contacts might be at the superior margin of the hippocampus. A polarity inversion occurred between RP 14 and RP 15 at the border of the anterior hippocampus. This positivity diminished in amplitude at more anterior MTL sites. A P300 was recorded simultaneously over the right parietal scalp with a similar onset as the anterior and posterior MTL positivities but which reached its peak somewhat earlier.

The MTL pattern for the visual x/o task shown in Figure 6 had the same features as described for auditory and somatic stimuli. The target ERP was marked by a positive potential at LP 9 located posterior to the hippocampus and by a large negative potential (−160 μV at 420 msec) at LP 10. At LP 16, in the amygdalar region, a positive potential was elicited by the target which had 2 peaks, one at 400 msec (which was also seen at LP 9) and another at 500 msec. ERPs from the right parietal scalp (P_4) obtained prior to implant surgery are presented at the top of the column. The scalp-recorded P300 overlapped substantially with the MTL ERPs. However, the positive ERP at

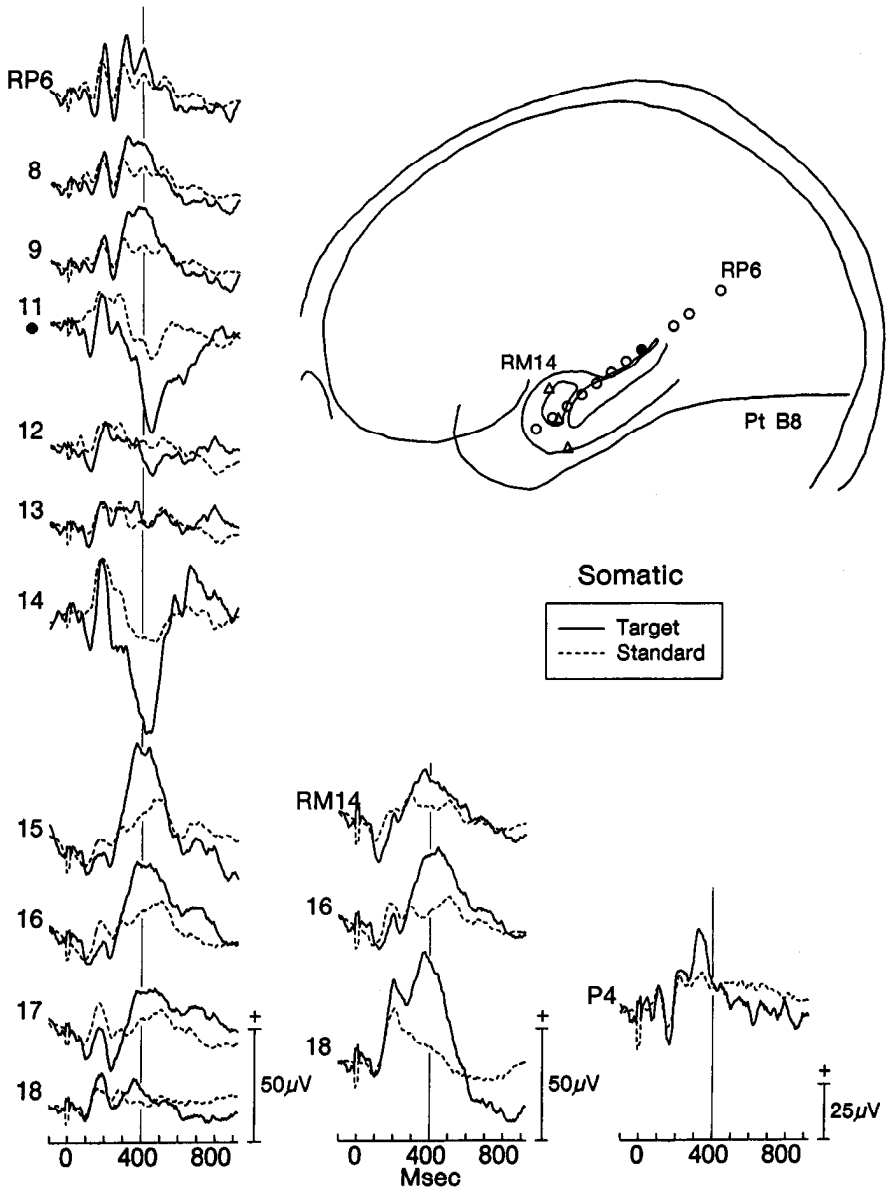

Figure 5. Scalp-recorded (P_4) and intracranial ERPs simultaneously elicited by right median nerve targets (*solid*) and left median nerve standards (*dashed*) for patient B8. Contacts from the RP probe are indicated by *circles* and contacts from the RM probe are indicated by *triangles*. RP 11 is depicted as a *filled circle*.

LP 9 reached its maximum earlier and the positive ERP at LP 16 reached its maximum later than scalp P300.

Figures 1–6 demonstrate the similarity of attended auditory, somatic, and visual target ERPs recorded from the MTL across patients. Figure 7 demonstrates that the spatial distribution of target ERPs was the same across modalities when tested *within* a patient. That is, the spatial gradients were the same across modalities. This can be seen in the leftmost 2 columns, where auditory and visual x/o task targets are presented for patient D20. MTL ERPs were recorded simultaneously with scalp recordings from a left parietal (P_3) scalp electrode. Posterior to the hippocampus at LP 9, positive ERPs were elicited by auditory and visual targets similar to those seen in Figures 1–7. At LP 10 at the posterior margin of the hippocampus, small negative potentials were seen which increased greatly in amplitude at LP 11 (−244 μV for auditory). Positive potentials were again obtained at LP 14, superior to the anterior hippocampus, and persisted until LP 17, near the amygdala, where they reached maximum amplitude.

This spatial pattern was also obtained for the NAMES task, a task in which the physical characteristics of the stimuli varied on each trial and in which a semantic distinction among the stimuli determined which was target and standard. The latencies of the components of the MTL target ERPs for visual names were much longer than those for auditory targets. For example, the peak latency of the negative potential at LP 11 for auditory stimuli was 380 msec, while for visual names it was 652 msec. Each component of the MTL pattern ERPs, however, shifted equivalently; i.e., the components covaried in latency.

The target ERPs from the NAMES task indicated that the MTL ERPs, like scalp-recorded P300, were not dependent upon physical stimulus features and could be elicited by abstract distinctions among stimuli. The independence of MTL potentials from physical stimulus properties was reaffirmed in the OMIT task, where the targets were nonoccurrences of regular auditory clicks. The target ERPs elicited in the OMIT task had the same spatial voltage profile as those elicited by stimulus presentations. As is typical for scalp-recorded P300s to stimulus omissions, the MTL

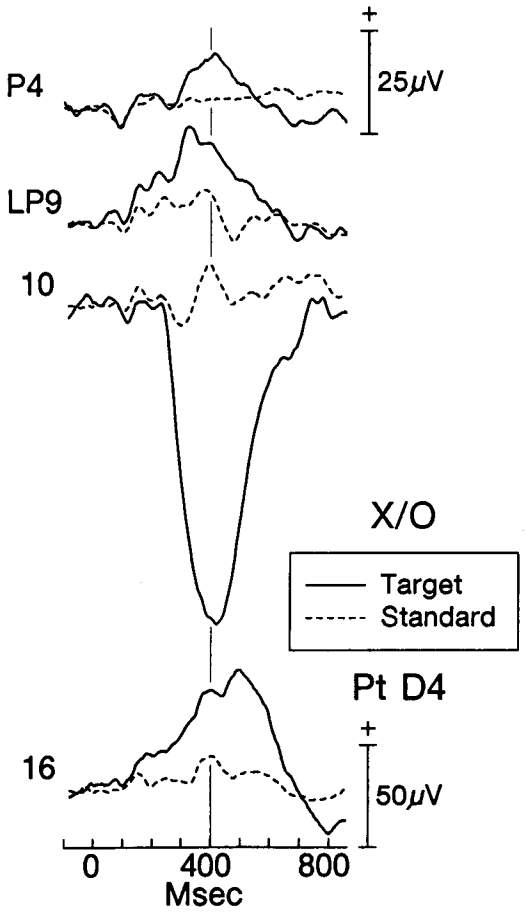

Figure 6. ERPs elicited by visual x/o targets (*solid*) and standards (*dashed*) from the LP probe in patient D4. The scalp ERP (P_4) was recorded prior to implant surgery and is plotted with a different amplitude calibration.

ERPs were smaller in amplitude and broader in waveshape than for stimulus presentations. This difference reflects both the variable time-locking of signal-averaging process to the decision that an omission occurred and the patient's reduced certainty that a target had indeed occurred (Ruchkin and Sutton, 1978).

Spatial distribution

The large negative potentials occurring in the vicinity of the hippocampus were the most frequently observed component of the MTL pattern, occurring in 54 of the 85 patients tested in the auditory task. In most cases, the MTL ERPs were elicited in all modalities tested; however, when testing was carried out over different days and when the patients were fatigued or uncomfortable, MTL ERPs were sometimes only clearly obtained during some runs or some testing sessions. Combining across modalities, this negative P300-like ERP was obtained in 61 of 88 patients (69%) with posterior–temporal probes.

The mean amplitude of the negative ERP for these 61 patients was -100 μV with a maximum amplitude of -250 μV. The mean latency to the maximum negativity was 428 msec. Scalp P300s were measured in 37 of these 61 patients in the same tasks prior to surgery. The mean amplitude of the maximum positive ERP at P_z was 16.3 μV, and its peak latency was 390 msec. Thus, on average, the MTL negative ERPs were 6 times larger than scalp-recorded P300s and about 40 msec later in peak latency.

The positive ERP occurring posterior and superior to the hippocampus was clearly observed in 33 patients in whom negative ERPs were also observed. Many patients also had positive ERPs in the absence of the negative ERP for reasons that will be considered further below. The mean amplitude of this positive ERP was 45 μV, with a maximum amplitude of 96 μV. The mean latency of the maximum positivity was 368 msec; however, this measure does not discriminate between the double positive peaks often obtained at these sites.

The positive ERP occurring anterior and inferior to the hippocampus was clearly observed in 43 patients in whom negative ERPs were also observed. As for the posterior positive ERP, many patients without negative ERPs also showed this positivity. The mean amplitude of this positive ERP was 48 μV, with a maximum amplitude of 113 μV. The mean latency to the maximum positivity was 433 msec, again ignoring multiple positive peaks.

The anatomical distribution of these 3 parts of the MTL pattern can be seen in Figure 8, where the position of the electrode from each patient at which the maximum amplitude of each ERP was obtained is indicated. Appropriate skull X-rays were not obtained in one patient, who is not included. It should be noted that in any patient ERPs could be obtained only along the probe track and that larger-amplitude ERPs might have been obtained at more optimal sites. It should also be emphasized that, in most patients, similar but somewhat smaller amplitude ERPs were also obtained at adjacent locations along the probe which are not shown. The posterior positivities cluster outside the most posterior aspect of the hippocampus, while the anterior positivities cluster at the anterior-most hippocampus, amygdala, and beyond. The large negative potentials were obtained for the most part from contacts which appear within the body of the hippocampus, although there are several contacts which appear to be located ventral to the hippocampus in the posterior parahippocampal gyrus.

Medial–lateral distribution

Unlike the lateral approach for electrode implantation used by other investigators (Halgren et al., 1980), our posterior approach did not allow a systematic study of the medial–lateral spatial gradient of the MTL ERPs. However, differences in probe placements across and within subjects provided limited information. As stated above, many patients from whom no large negative MTL ERPs were obtained nevertheless had robust anterior and/or posterior positive ERPs. In several cases, such as that illustrated in Figure 9, the posterior–temporal probe appeared not to penetrate the hippocampus but passed slightly lateral to it. In such cases, positive ERPs were obtained at all contacts along the probe. It can be seen that the waveshapes of the positivities changed continuously from the most posterior (RP 7) to most anterior contacts as the positivity broadened and increased in amplitude. This broadening appeared due to the addition of a second positive potential at about the latency of the isolatency line which was barely present at RP 9 but which increased in amplitude at more anterior contacts.

Other data suggest that a medial–lateral potential gradient may contribute to the polarity inversion often observed near the posterior hippocampus. Figure 10*A* presents ERPs from contacts LP 10 and RP 10 from patient W19 which appeared identically placed in sagittal view. ERPs are shown for auditory,

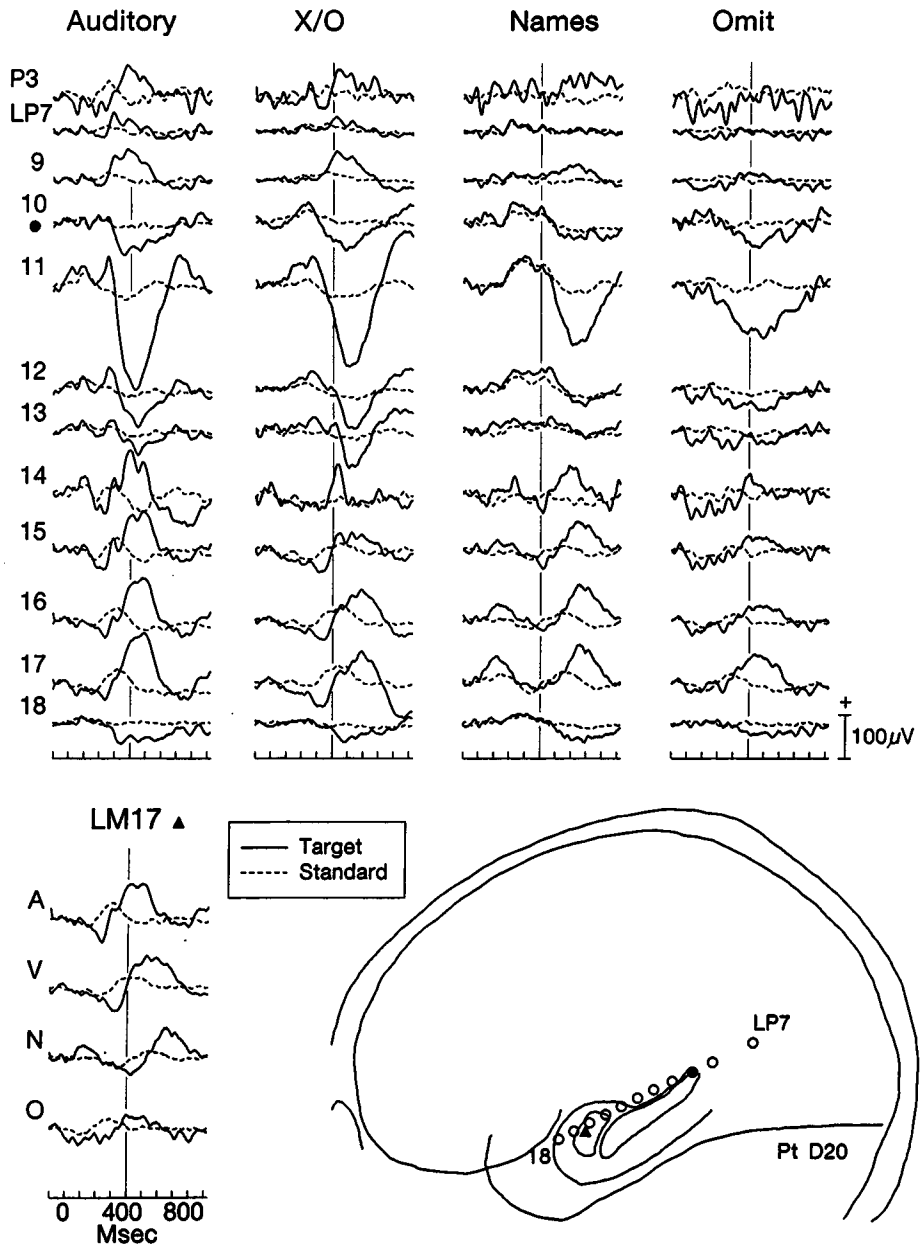

Figure 7. ERPs elicited by targets (*solid*) and standards (*dashed*) from auditory COUNT, visual X/O, NAMES, and auditory OMIT tasks in patient D20. A scalp-recorded ERP recorded simultaneously with the intracranial ERPs (P_3) is shown at the top of each column. A comparison of all 4 tasks is shown at the *lower left* for contact LM 17 located within the amygdala. Contacts from the LP probe are indicated as *circles* with LP 10 depicted as a *filled circle*. LM 17 is depicted as a *filled triangle*.

visual X/O, and NAMES tasks. Scalp-recorded ERPs obtained prior to surgery for the same tasks are also plotted for left (P_3) and right (P_4) parietal scalp locations. For both visual tasks, ERPs elicited by standards are overplotted, while for the auditory task, ERPs elicited by ignored targets are drawn. The counted targets from all tasks elicited large negative ERPs at LP 10, while simultaneously large positive ERPs were elicited at RP 10. In coronal sections, electrode locations were too close to accurately determine whether they were inside or outside of the C-shaped semicylinder formed by the posterior hippocampus. However, in view of the ERPs shown in Figure 9 above, the data suggest that RP 10 was medial to the hippocampus, while LP 10 was within. Note that despite differences in polarity, both the negative and positive MTL ERPs covaried in latency across tasks.

Large negative ERPs were recorded from both RP 12 and LP 12 (Fig. 10*B*), where electrode estimates from coronal sections placed each unambiguously within the hippocampus. The positive–negative transition from RP 10 to RP 12 suggests that a polarity inversion occurred as the probes crossed from outside to inside of the hippocampus.

Sequential dependencies

The amplitude of scalp-recorded P300 in categorization tasks is dependent upon the sequence of the immediately preceding stimuli (Squires et al., 1976a). Sequential dependencies were examined for MTL ERPs in patients in whom single-trial ERPs were available for off-line sorting. Figure 11 presents a sequential analysis of data from the somatic COUNT task for patients B1 and B10. The ERPs elicited by targets which were immediately preceded by standards were largest in amplitude. The MTL negativity was reduced if the target was preceded by another target. Standards preceded by other standards were associated with the smallest amplitude MTL negativities. However, a stan-

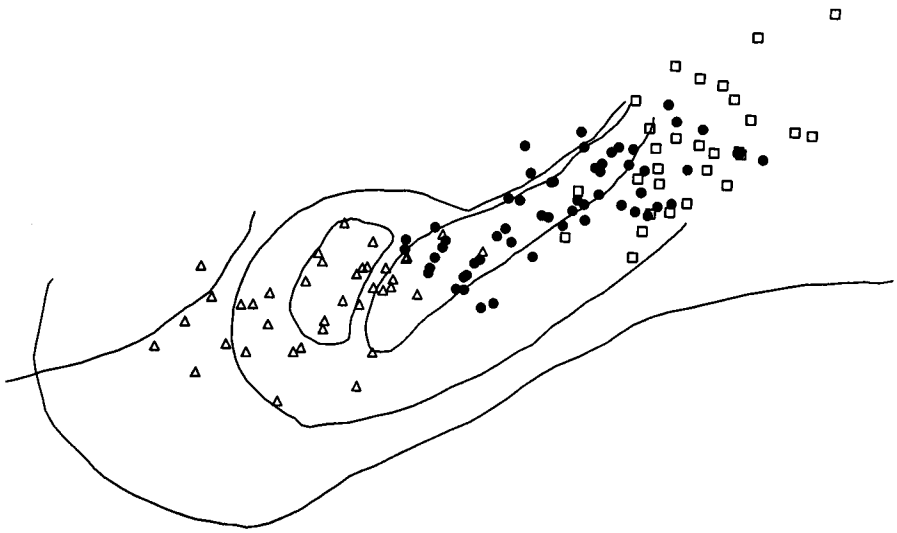

Figure 8. Summary of contact locations from which maximum amplitude MTL ERPs were obtained from each patient. The contacts from which negative MTL ERPs were obtained are shown as *filled circles.* The contacts from which the posterior positive and anterior positive ERPs were obtained are shown as *open squares* and *triangles,* respectively. Posterior and anterior positive potentials are indicated only for those patients from whom a negative MTL ERP was also obtained.

dard preceded by a target was associated with an increased amplitude MTL negativity. Thus, for attended stimuli, repetitions of the same stimulus reduced the amplitude of the MTL negative ERP, while a nonrepeating stimulus increased its amplitude.

Figure 12 displays ERPs to standards from patient B8 (see inset of Fig. 5 for electrode locations) for auditory and somatic COUNT task and NAMES task. As in Figure 11, ERPs elicited by standards which were immediately preceded by another standard had small MTL potentials. ERPs elicited by standards immediately preceded by targets were larger in amplitude as shown before, and, for this patient, this enhancement was seen for all 3 parts of the MTL pattern. Sequential effects were also seen for the NAMES, which is notable in that it dissociates the effect from the repetition of physically identical stimuli. Each visual name is physically different from the preceding, regardless of category membership. Thus, the sequential effect depends at least in part upon categorization independent of physical identity.

Discussion

Halgren and colleagues (Halgren et al., 1980, 1986; Squires et al., 1983; Smith et al., 1986; Stapleton and Halgren, 1987) have reported what they termed "endogenous limbic potentials" (ELPs) from the medial temporal region elicited by target stimuli in auditory and visual oddball tasks and by stimulus omissions. They concluded that these potentials were locally generated in the hippocampus. The present results extend these findings, as well as our own preliminary work (Wood et al., 1980, 1984; McCarthy et al., 1982) based upon smaller patient samples.

Neural generators

The MTL ERPs appeared in a fairly stereotypic spatial pattern when sampled by a multicontact probe following a path along the long axis of the hippocampus. As summarized in Figure 8, sharp voltage gradients to target ERPs were observed among contacts posterior to the hippocampus (positive) to contacts near the body of the hippocampus (negative) and again to contacts anterior to the hippocampus in the region of the amygdala (positive). Sharp gradients were also seen (Fig. 10) at the lateral margin of the hippocampus. Such medial–lateral gradients have been described by Stapleton and Halgren (1987, their figure 5) in recordings from multicontact depth probes aimed at the hippocampus from the lateral scalp.

The spatial distribution of the MTL ERPs along the depth probes suggests that the probe enters and then exits an enclosed region of negative extracellular potential. The relatively restricted distribution of the negative ERP and its larger amplitude compared with the posterior and anterior positive ERPs can be accounted for by the C-shaped semicylinder formed by the hippocampal pyramidal cells. The radial arrangement of pyramidal neurons with their apical dendrites oriented inward would result in larger field potentials within the cylinder than outside (Klee and Rall, 1977).

Converging data indicating the relationship of these negative MTL ERPs to hippocampal neurons have come from neuropathological study of the excised medial temporal lobes. In many patients, the MTL ERPs are absent or greatly attenuated in the epileptogenic temporal lobe (Squires et al., 1983; McCarthy et al., 1987; Meador et al., 1987). It has been demonstrated previously that the hippocampus in such patients shows considerable cell loss (Babb et al., 1984), as well as marked biochemical abnormalities (Partington et al., 1986). However, in some patients, particularly those found to have temporal lobe tumors, hippocampal pathology is less severe. We have demonstrated a correlation of 0.72 between hippocampal cell loss and abnormalities in the MTL negative ERP (Wood et al., 1988). However, the high intercorrelation of cell loss from each of the subfields measured (0.6–0.8) does not permit a more precise specification of which hippocampal subfields are critical in generating the MTL negativity.

The synaptic events underlying these task-dependent field potentials are uncertain. Negative extracellular potential within and positive extracellular potential outside of the semicylinder formed by the pyramidal cells of the hippocampus could result from (1) depolarization of the distal apical dendrites and associated passive outward current flow from the cell bodies and basal dendrites, or (2) hyperpolarization near the cell bodies creating a current sink (and negative extracellular potential) at the distal apical dendrites. Considerable evidence exists for synchronized distal EPSPs and proximal IPSPs in hippocampal physiology (see Schwartzkroin and Mueller, 1987), the former by excitatory input in the molecular layer from the perforant pathway and the latter from recurrent inhibition mediated by interneurons synapsing near the soma. In either case, electrodes

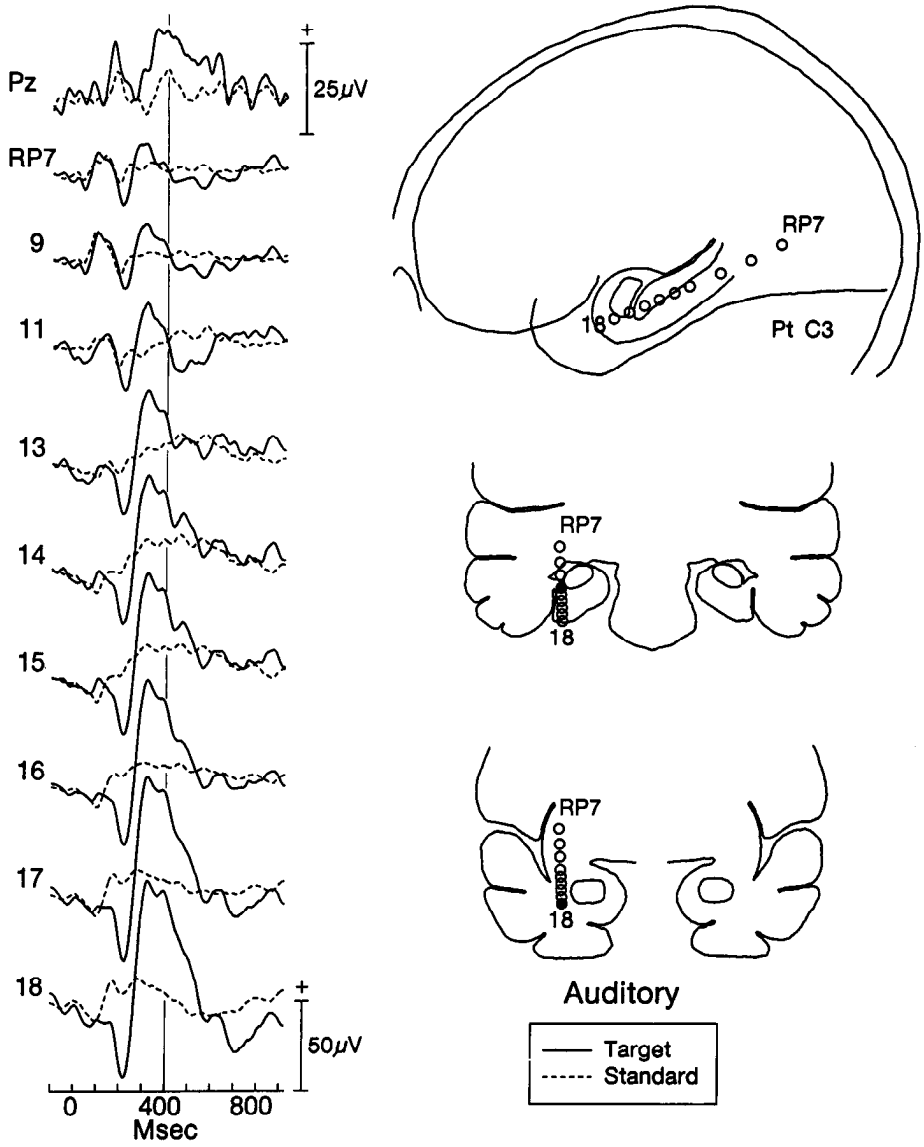

Figure 9. Auditory COUNT target (*solid*) and standard (*dashed*) ERPs in patient C3. A scalp-recorded ERP obtained simultaneously is shown at the top of the column (note different voltage calibration). Contacts from the RP probe are indicated as *circles* on the *upper insert* depicting a sagittal view of the brain. The positions of these same contacts are shown in coronal views at the level of the posterior hippocampus and amygdala. The *filled circles* indicate the contact in the coronal plane: RP 13 at the posterior hippocampus and RP 18 at the amygdala.

lateral and dorsal to the hippocampus would record summated positive synaptic potentials, while electrodes within the enclosed hippocampus would record negative synaptic potentials. Thus, our present field potential distributions are insufficient to determine their underlying synaptic basis. Halgren et al. (1986) noted that the typical slow wave following hippocampal spikes is negative within the hippocampus, where ELPs are negative, and positive outside of the hippocampus and at the scalp. Assuming on the basis of animal data that these epileptiform slow waves represent primarily summated IPSPs, Halgren and colleagues suggested that ELPs with similar potential distributions may reflect inhibitory processes in the hippocampus. While suggestive, these findings are not conclusive and require more direct evidence, perhaps in animal models of these endogenous ERPs.

To summarize, our tentative model for the generation of the negative MTL ERP suggests that the positive ERPs recorded medial and dorsal to the hippocampus reflect outward source currents from the same neuronal elements in which the negative ERPs represent inward currents. Thus, both positive and negative ERPs are expected from the dipolar arrangement of pyramidal cells. As the anterior hippocampus rotates caudomedially in the uncus, this dipolar field would be oriented anteriorly at the genu. Positive ERPs would be expected in the region of the amygdala, as have been observed. The narrowing and ascension of the semicylinder in the posterior hippocampus would have a similar effect, with the dipolar field pointing posteriorly. Thus, to a first approximation, this simple model explains the major features of the MTL spatial pattern.

While some aspects of this model are likely correct, the sometimes large differences in waveform morphologies and latencies present in MTL pattern argue that this initial model may not be complete. It is likely that the convoluted anatomy of the uncal hippocampus could account for considerable waveform variability in the anterior MTL. However, we have often observed multiple positive peaks posterior and dorsal to the hippocampus with the earlier positive peak occurring before the negative ERP in the hippocampus. Thus, other generators contribute to this positive ERP in addition to the hippocampus. Our model also does not consider the contribution of neurons within the parahippocampal gyrus and entorhinal area, regions presumably active during this task.

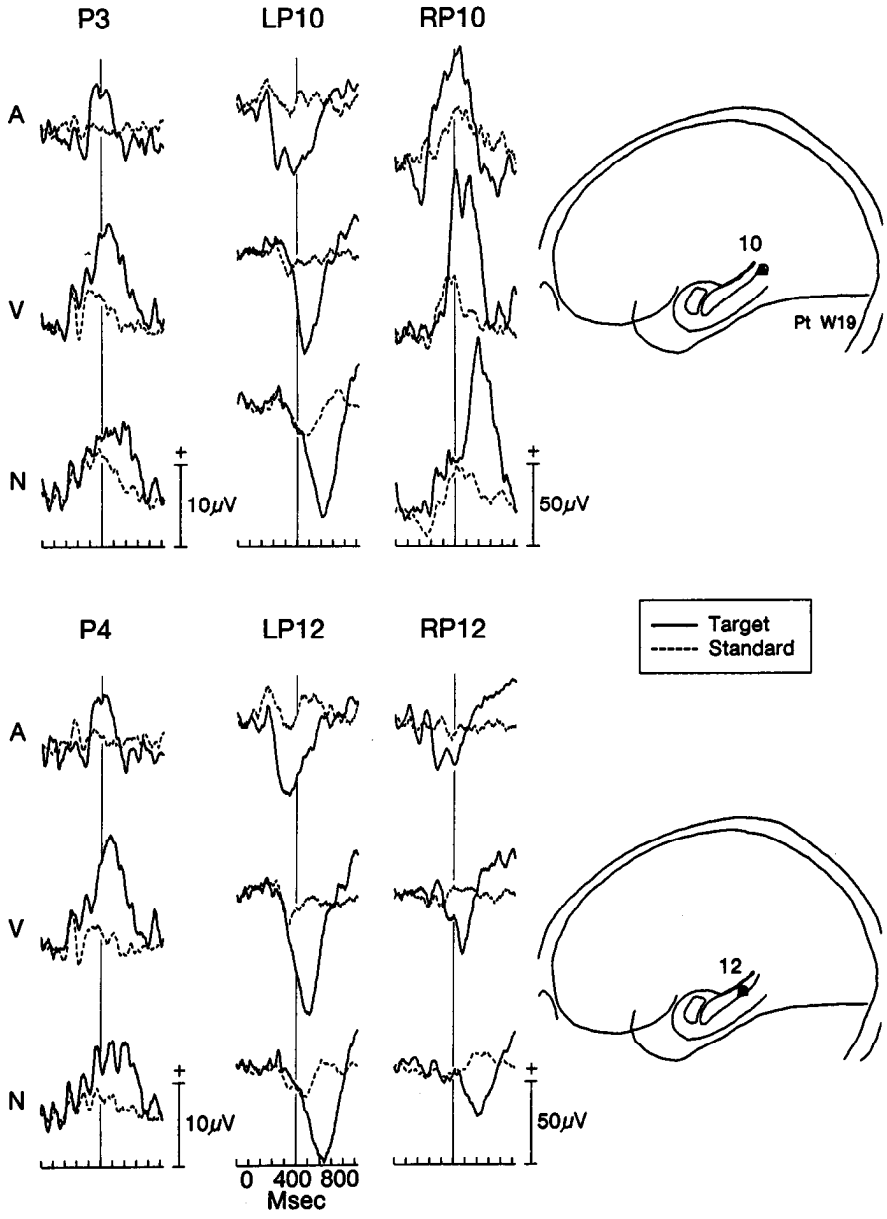

Figure 10. Top, Target (*solid*) and standard (*dashed*) ERPs for auditory COUNT (*A*), X/O, and NAMES (*N*) tasks for patient W19. ERPs are shown for a left parietal scalp electrode (P_3) acquired prior to implant surgery and from RP and LP 10 (*open circle* and *filled triangle,* respectively). *Bottom,* Target and standard ERPs as plotted above from the right parietal (P_4) scalp and from contacts RP 12 and LP 12 (*open circle* and *filled triangle,* respectively).

Relationship to scalp-recorded P300

The MTL ERPs elicited in the hippocampus have many similar properties to scalp P300 recorded in the same tasks. The MTL target ERPs were elicited by stimuli of all modalities, but only when the stimuli were task-relevant. Identical sequences of stimuli did not elicit MTL ERPs when the stimuli were irrelevant and patients were instructed to ignore them. Thus, MTL ERPs do not reflect obligatory sensory processing, but rather some aspect of neural processing associated with the task. That MTL ERPs can be elicited by stimulus omissions further emphasizes the dissociation of these potentials from the exogenous properties of the stimulus, as well as confirming their dependence upon *endogenous* neural processes.

The sensitivity to the preceding sequence of stimuli provides evidence that these ERPs are not solely dependent upon the subject's covert response to the target stimulus. This suggests that these endogenous ERPs are sensitive to expectancies that subjects develop based on the immediate stimulus sequence (Squires et al., 1976a), or perhaps to a change in response set occasioned by the stimulus. Sequential effects may also result from habituation to a repeating stimulus and dishabituation caused by a stimulus change. It is unlikely that the MTL ERPs reflect stimulus habituation if this process is based only upon physical stimulus properties since large MTL ERPs were elicited by exemplars of the category of male's names, even though different physical stimuli were presented on each trial. Sequential effects were also observed in the NAMES task (Fig. 12).

The latency of the MTL ERPs varied across task conditions, being shortest for auditory and somatic tasks, intermediate for the visual X/O task, and longest for NAMES. The latency of scalp P300 has been found to covary with the time required to categorize stimuli with the latency of single, unaveraged P300s positively correlated with reaction time (Kutas et al., 1977). The increased peak latency of the MTL ERPs in the NAMES task was accompanied by an increase in its onset latency. This suggests

that the neural activity reflected by these MTL ERPs occurred subsequent to the identification of the stimulus category, that is, the MTL was responding to highly preprocessed sensory input in which the stimulus was abstracted into a meaningful event on the basis of task instructions.

Our results and those of Halgren and collaborators (Halgren et al., 1980; Stapleton and Halgren, 1987) establish a close correspondence between the characteristics of scalp P300 and the MTL ERPs in categorization tasks. Given the interest in developing noninvasive probes of brain function in the assessment of disease, it is important to know to what extent the scalp P300 represents volume-conducted potentials from the MTL. A strong contribution of MTL field potentials to the scalp would allow inferences to be made about the integrity of this area, much in the manner that scalp-recorded short-latency evoked potentials are used clinically in determining the integrity of afferent pathways. The problem with identifying particular ERPs with particular intracranial generators is that the ERPs reflect a spatially weighted sum of all time-locked extracellular potentials. This problem of the superimposition of coactive generators is exacerbated in scalp recordings, where the distances from the active generators are great and where the resistive properties of the skull and scalp reduce the spatial resolution of the recordings. Spatially restricted deep generators can produce broad scalp potential fields which are indistinguishable from extended superficial sources.

If the MTL ERPs contribute significantly to the scalp P300 distribution, and if these MTL ERPs are reduced or absent in the epileptogenic hemisphere, then corresponding changes should be observed at the scalp in patients with focal temporal lobe seizures. In several patients (McCarthy et al., 1987), a large asymmetry in the scalp distribution of P300 was found in which amplitudes over the far lateral temporal scalp (typically T_3/T_4) ipsilateral to the focal hemisphere were reduced. Smaller asymmetries in P300 area over this region characterized the larger patient sample. Despite these lateral asymmetries, however, the maximum amplitude of the P300 typically remained at the midline.

Unilateral temporal lobectomy does not alter the scalp distribution of P300 in the manner expected if bilateral hippocampal generators were its sole generators (Wood et al., 1982; Johnson and Fedio, 1984; Stapleton and Halgren, 1987). Studies of P300 analogs from the skull in nonhuman primates with bilateral hippocampal lesions have also indicated that midline P300 is unaffected by the lesions (Paller et al., 1988). We have noted, however, that the amplitude and, especially, duration of P300 over the lateral temporal scalp ipsilateral to the lesion is reduced compared with presurgical recordings and compared with the contralateral scalp postsurgically when recorded against a noncephalic reference. Thus, unilateral temporal lobectomy (which in our patients is limited to the medial temporal lobe and anterior pole sparing most of temporal neocortex) can produce scalp asymmetries or exaggerate existing asymmetries, but primarily at the lateral temporal scalp, where P300 amplitude is relatively small. This indicates that other generators must account for the remainder of the P300 scalp distribution, particularly at the midline, where it is largest in amplitude. Generators in frontal cortex and other regions may also contribute to scalp P300 (McCarthy and Wood, 1987). The relationship of these cortical generators to those in the MTL will be considered in a subsequent paper.

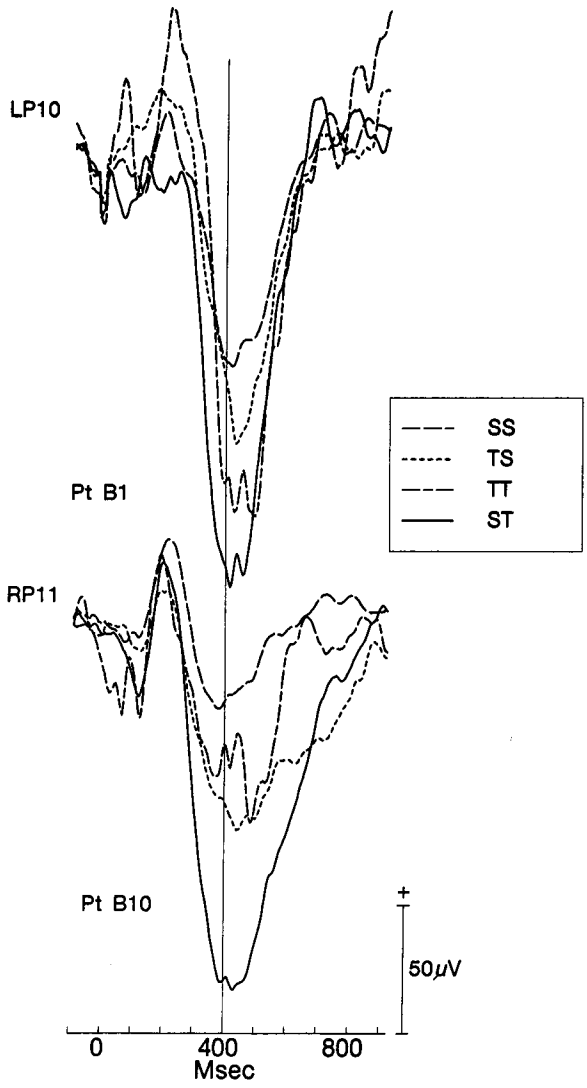

Figure 11. ERPs elicited by somatic stimuli for RP 11 for patient B1 (*top*) and LP 10 for patient B10 (*bottom*). The ERPs were selectively averaged as a function of the preceding stimulus. *SS,* Standards preceded by standards (*long dash*), *TS,* Standards preceded by targets (*short dash*), *TT,* Targets preceded by targets (*chain dash*), *ST,* Targets preceded by standards (*solid*).

Patient variability

The MTL pattern was observed in most patients. However, in some patients, the pattern was missing in part or whole. Three factors appear important in accounting for individual variation in these potentials.

1. We and others (Squires et al., 1983; Meador et al., 1987) have often found a diminution or absence of endogenous MTL potentials in the hemisphere determined to be the site of the epileptogenic lesion. In some cases (such as patient T10 in Fig. 4), a more restricted alteration in the MTL pattern appeared to correlate with the location of abnormal tissue. Of the 27 patients in whom no focal MTL negativities were found, 17 had only a single posterior–temporal probe implanted in the focal hemisphere.

2. As is obvious from the sharp amplitude gradients in the data discussed above, the probe trajectory through the MTL and the corresponding contact locations affect both the ampli-

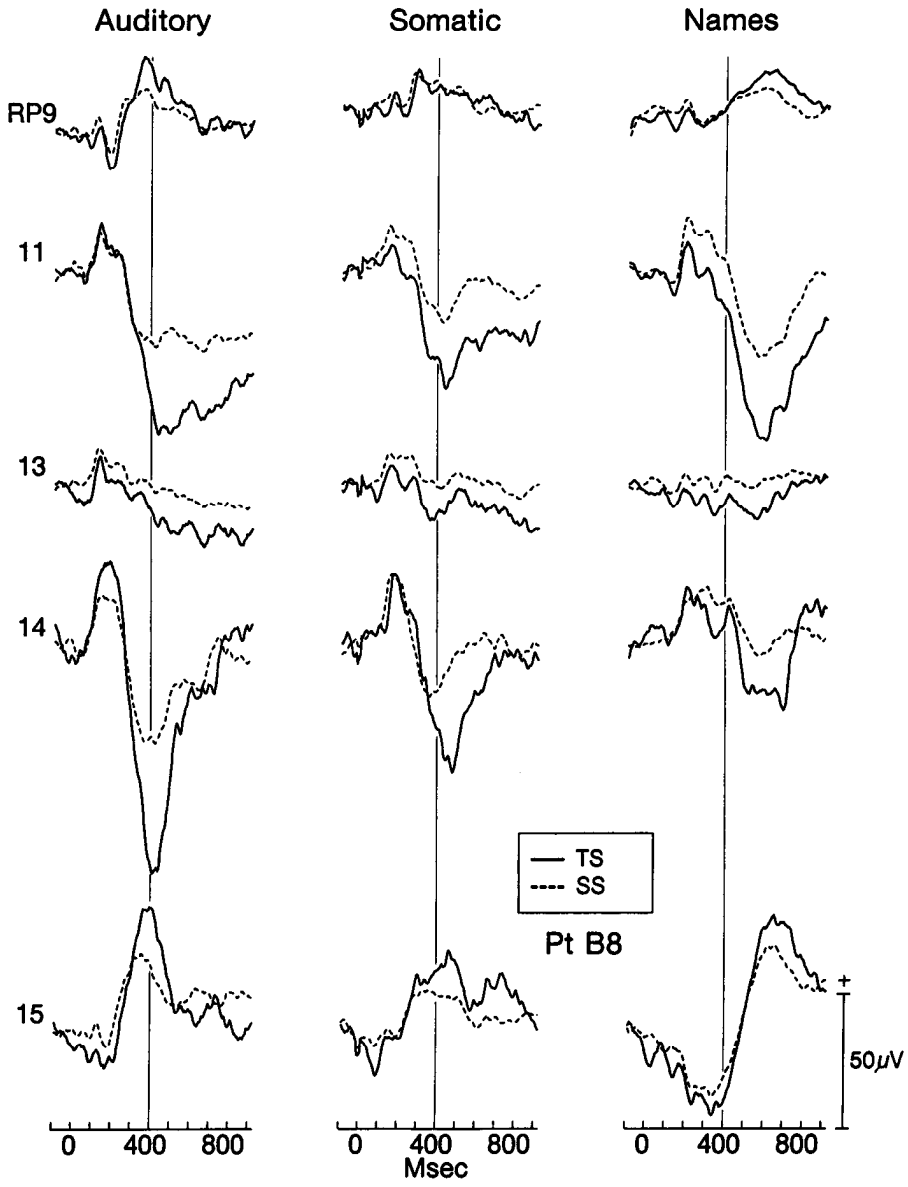

Figure 12. ERPs elicited by auditory, somatic, and visual names standards from contacts along the RP probe of patient B8 (see inset of Fig. 5 for contact locations). ERPs elicited by standards preceded by targets (*TS: solid*) are compared with standards preceded by other standards (*SS: dashed*).

tude and polarity of the MTL potentials. In some patients, altered amplitudes and waveshapes appeared likely due to the probe missing the hippocampus either laterally (Fig. 9) or dorsally. Four of the patients without focal MTL negativities had probes which clearly missed the hippocampus laterally.

3. The subjective state of the patient affected the amplitude of the MTL potentials. Best results were obtained from alert, motivated patients. Patients who were uncomfortable or fatigued often did not produce large MTL potentials despite accurate counts of target stimuli (see also Squires et al., 1983). Major differences in the amplitude of endogenous MTL potentials occurred in one patient in which a retest was performed 2 d after initial testing was discontinued due to fatigue. Small and poorly defined MTL potentials were recorded in the first session, while large focal MTL potentials were obtained in the second session when the patient was alert and highly cooperative.

The weakest aspect of our and other intracranial studies is the imprecise localization of the electrode contacts with respect to anatomical structures. While quite adequate for implicating the MTL and the hippocampus in particular in the generation of P300-like potentials, localization is inadequate for testing more detailed source models. Magnetic resonance imaging (MRI) is now employed in the placement of depth probes. This technique allows a more accurate assessment of probe trajectories with respect to an individual patient's neuroanatomy (Zhang et al., 1988). Depth electrodes composed of materials which can be safely imaged with MRI are now being introduced.

References

Allison, T., C. C. Wood, and G. McCarthy (1986) The central nervous system. In *Psychophysiology: Systems, Processes, and Applications: A Handbook,* E. Donchin, S. Porges, and M. Coles, eds., pp. 5–25, Guilford Press, New York.

Arthur, D. L., and A. Starr (1984) Task-relevant late positive component of the auditory event-related potential in monkeys resembles P300 in humans. Science *223:* 186–188.

Babb, T. L., W. J. Brown, J. Pretorius, C. Davenport, J. P. Lieb, and P. H. Crandall (1984) Temporal lobe volumetric cell densities in temporal lobe epilepsy. Epilepsia *25:* 729–740.

Buchwald, J. S., and N. K. Squires (1981) Endogenous auditory potentials in the cat: A P300 model. In *Conditioning: Representation of Involved Neural Function,* C. Woody, ed., Raven, New York.

Courchesne, E., R. Elsmasian, and R. Y. Courchesne (1987) Electrophysiological correlates of cognitive processing: P3b and Nc, basic, clinical, and developmental research. In *A Textbook of Clinical Neurophysiology,* A. M. Halliday, S. R. Butler, and R. Paul, eds., pp. 645–676, Wiley, New York.

Darcey, T. M., and P. D. Williamson (1985) Spatio-temporal EEG measures and their application to human intracranially recorded seizures. Electroencephalogr. Clin. Neurophysiol. *61:* 573–587.

Desmedt, J. E. (1980) P300 in serial tasks: An essential post-decision closure mechanism. Prog. Brain Res. *24:* 682–686.

Donchin, E. (1981) Surprise! . . . Surprise? Psychophysiology *18:* 493–513.

Donchin, E., and M. G. H. Coles (1988) Is the P300 component a manifestation of context updating? Behav. Brain Sci. *11:* 357–374.

Friedman, D., H. G. Vaughan, Jr., and L. Erlenmeyer-Kimling (1981) Multiple late positive potentials in two visual discrimination tasks. Psychophysiology *18:* 635–649.

Gabriel, M., S. P. Sparenborg, and E. Donchin (1983) Macropotentials recorded from the cingulate cortex and anterior thalamus in rabbits during the "oddball" paradigm used to elicit P300 in humans. Soc. Neurosci. Abstr. *9:* 1200.

Goodin, D. S., K. C. Squires, and A. Starr (1978) Long latency event-related components of the auditory evoked potential in dementia. Brain *101:* 635–648.

Goodin, D. S., A. Starr, T. Chippendale, and K. C. Squires (1983) Sequential changes in the P3 component of the auditory evoked potential in confusional states and dementing illnesses. Neurology *33:* 1215–1218.

Halgren, E., N. K. Squires, C. L. Wilson, J. W. Rohrbaugh, T. L. Babb, and P. H. Crandall (1980) Endogenous potentials generated in the human hippocampal formation and amygdala by infrequent events. Science *210:* 803–805.

Halgren, E., J. Engel, Jr., C. L. Wilson, R. D. Walter, N. K. Squires, and P. H. Crandall (1983) Dynamics of the hippocampal contribution to memory: Stimulation and recording studies in humans. In *Neurobiology of the Hippocampus,* W. Seifert, ed., pp. 529–572, Academic, London.

Halgren, E., J. M. Stapleton, M. Smith, and I. Altafullah (1986) Generators of the human scalp P3(s). In *Evoked Potentials,* R. Q. Cracco and I. Bodis-Wollner, eds., pp. 269–284, Liss, New York.

Johnson, R., and P. Fedio (1984) ERP and P300 activity in patients following unilateral temporal lobectomy. Soc. Neurosci. Abstr. *10:* 846.

Klee, M., and W. Rall (1977) Computed potentials of cortically arranged populations of neurons. J. Neurophysiol. *40:* 647–666.

Kutas, M., G. McCarthy, and E. Donchin (1977) Augmenting mental chronometry: The P300 as a measure of stimulus evaluation time. Science *197:* 792–795.

McCarthy, G., and E. Donchin (1981) A metric for thought: A comparison of P300 latency and reaction time. Science *211:* 77–80.

McCarthy, G., and E. Donchin (1983) Chronometric analysis of human information processing. In *Advances in Psychology, Vol. 10, Tutorials in Event Related Potential Research: Endogenous Potentials,* A. W. K. Gaillard and W. Ritter, eds., pp. 251–268, North-Holland, Amsterdam.

McCarthy, G., and C. C. Wood (1987) Intracranial recordings of endogenous ERPs in humans. In *The London Symposia, EEG Supplement 39,* R. J. Ellingson, N. M. F. Murray, and A. M. Halliday, eds., pp. 331–337, Elsevier, London.

McCarthy, G., C. C. Wood, T. Allison, W. R. Goff, P. D. Williamson, and D. D. Spencer (1982) Intracranial recordings of event-related potentials in humans engaged in cognitive tasks. Soc. Neurosci. Abstr. *8:* 976.

McCarthy, G. M., T. M. Darcey, C. C. Wood, P. D. Williamson, and D. D. Spencer (1987) Asymmetries in scalp and intracranial endogenous ERPs in patients with complex partial epilepsy. In *Fundamental Mechanisms of Human Brain Function,* J. Engel, Jr., G. A. Ojemann, H. O. Luders, and P. D. Williamson, eds., pp. 51–59, Raven, New York.

Meador, K. J., D. W. Loring, D. W. King, B. B. Gallagher, M. J. Gould, H. F. Flanigin, and J. R. Smith (1987) Limbic evoked potentials predict site of epileptic focus. Neurology *37:* 494–497.

Mitzdorf, U. (1985) Current source-density method and application in cat cerebral cortex: Investigation of evoked potentials and EEG phenomena. Physiol. Rev. *65:* 37–100.

Neville, H. J., and S. L. Foote (1984) Auditory event-related potentials in the squirrel monkey: Parallels to human late wave responses. Brain Res. *298:* 107.

Nicholson, C., and J. A. Freeman (1975) Theory of current-source-density analysis and determination of conductivity tensor for anuran cerebellum. J. Neurophysiol. *38:* 356–369.

Paller, K. A., S. Zola-Morgan, L. R. Squire, and S. A. Hillyard (1988) P3-like brain waves in normal monkeys and monkeys with medial temporal lesions. J. Behav. Neurosci. *102:* 714–725.

Partington, J. P., N. C. de Lanerolle, J. Madl, and D. D. Spencer (1986) Glutamate immunoreactivity in the mammalian hippocampus: Changes in human epileptogenic hippocampus. Soc. Neurosci. Abstr. *12:* 382.

Pfefferbaum, A., J. M. Ford, B. G. Wenegrat, W. T. Roth, and B. S. Kopell (1984) Clinical application of the P3 component of event-related potentials. I. Normal aging. Electroencephalogr. Clin. Neurophysiol. *59:* 85–103.

Polich, J. (1984) P300 latency reflects the cognitive effects of personal drinking history in normals and individuals at risk for alcoholism. Psychophysiology *21:* 592–593.

Polich, J., C. L. Ehlers, S. Otis, A. J. Mandell, and F. E. Bloom (1986) P300 latency reflects the degree of cognitive decline in dementing illness. Electroencephalogr. Clin. Neurophysiol. *63:* 138–144.

Rohrbaugh, J. W., K. Syndulko, and D. B. Lindsley (1978) Cortical slow negative waves following non-paired stimuli: Effects of task factors. Electroencephalogr. Clin. Neurophysiol. *45:* 551–567.

Roth, W. T., T. B. Horvath, A. Pfefferbaum, and B. S. Kopell (1980) Event-related potentials in schizophrenia. Electroencephalogr. Clin. Neurophysiol. *48:* 127–139.

Ruchkin, D. S., and S. Sutton (1978) Equivocation and P300 amplitude. In *Multidisciplinary Perspectives in Event-Related Brain Potential Research,* D. A. Otto, ed., pp. 175–177, U.S.G.P.O., Washington, D.C.

Ruchkin, D. S., S. Sutton, and M. Stega (1980) Emitted P300 and slow wave event-related potentials in guessing and detection tasks. Electroencephalogr. Clin. Neurophysiol. *49:* 1–14.

Schwartzkroin, P. A., and A. L. Mueller (1987) Electrophysiology of hippocampal neurons. In *Cerebral Cortex, Vol. 6, Further Aspects of Cortical Function, Including Hippocampus,* E. G. Jones and A. Peters, eds., pp. 295–343, Plenum, New York.

Simson, R., H. G. Vaughan, Jr., and W. Ritter (1977) The scalp topography of potentials in auditory and visual discrimination tasks. Electroencephalogr. Clin. Neurophysiol. *42:* 528–535.

Smith, M. E., J. M. Stapleton, and E. Halgren (1986) Human medial temporal lobe potentials evoked in memory and language tasks. Electroencephalogr. Clin. Neurophysiol. *63:* 145–159.

Spencer, S. S., D. D. Spencer, P. D. Williamson, and R. H. Mattson (1982) The localizing value of depth electroencephalography in 32 refractory patients. Ann. Neurol. *12:* 248–253.

Squires, K. C., C. Wickens, N. K. Squires, and E. Donchin (1976a) The effect of stimulus sequence on the waveform of the cortical event-related potential. Science *193:* 1142–1146.

Squires, K. C., E. Donchin, R. I. Herning, and G. McCarthy (1976b) On the influence of task relevance and stimulus probability on event-related potential components. Electroencephalogr. Clin. Neurophysiol. *42:* 1–14.

Squires, N. K., K. C. Squires, and S. A. Hillyard (1975) Two varieties of long-latency positive waves evoked by unpredictable auditory stimuli in man. Electroencephalogr. Clin. Neurophysiol. *38:* 387–401.

Squires, N. K., E. Halgren, C. Wilson, and P. Crandall (1983) Human endogenous limbic potentials: Cross-modality and depth/surface comparisons in epileptic subjects. In *Tutorials in ERP Research: Endogenous Components,* A. W. K. Gaillard and W. Ritter, eds., pp. 217–232, North Holland, Amsterdam.

Stapleton, J. M., and E. Halgren (1987) Endogenous potentials evoked in simple cognitive tasks: Depth components and task correlates. Electroencephalogr. Clin. Neurophysiol. *67:* 44–52.

Sutton, S., M. Braren, J. Zubin, and E. R. John (1965) Evoked potential correlates of stimulus uncertainty. Science *150:* 1187–1188.

Sutton, S., P. Tueting, J. Zubin, and E. R. John (1967) Information delivery and the sensory evoked potential. Science *155:* 1436–1439.

Talairach, J., and G. Szikla (1967) *Atlas of Stereotaxic Anatomy of the Telencephalon,* Masson, Paris.

Verleger, R. (1988) Event-related potentials and cognition: A critique of the context updating hypothesis and an alternative interpretation of P3. Behav. Brain Sci. *11:* 343–356.

Wilder, M. B., G. R. Farley, and A. Starr (1981) Endogenous late

positive component of the evoked potential in cats corresponding to P300 in humans. Science *211:* 605–607.

Williamson, P. D., D. D. Spencer, S. S. Spencer, and R. H. Mattson (1980) Presurgical intensive monitoring using depth electroencephalography in temporal lobe epilepsy. In *Advances in Epileptology: The Xth Epilepsy International Symposium,* J. A. Wada and J. K. Penry, eds., pp. 73–81, Raven, New York.

Wood, C. C., and T. Allison (1981) Interpretation of evoked potentials: A neurophysiological perspective. Canad. J. Psychol. *35:* 113–135.

Wood, C. C., T. Allison, W. R. Goff, P. D. Williamson, and D. D. Spencer (1980) On the neural origin of P300 in man. In *Progress in Brain Research, Vol. 54: Motivation, Motor, and Sensory Processes of the Brain: Electrical Potentials, Behavior and Clinical Use,* H. H. Kornhuber and L. Deecke, eds., pp. 51–56, Elsevier, Amsterdam.

Wood, C. C., G. McCarthy, T. Allison, W. R. Goff, P. D. Williamson, and D. D. Spencer (1982) Endogenous event-related potentials following temporal lobe excisions in humans. Soc. Neurosci. Abstr. *8:* 976.

Wood, C. C., G. McCarthy, J. H. Kim, D. D. Spencer, and P. D. Williamson (1988) Abnormalities in temporal lobe event-related potentials predict hippocampal cell loss in temporal lobe epilepsy. Soc. Neurosci. Abstr. *14:* 5.

Wood, C. C., G. McCarthy, N. K. Squires, H. G. Vaughan, D. L. Woods, and W. C. McCallum (1984) Anatomical physiological substrates of event-related potentials. Ann. NY Acad. Sci. *425:* 681–721.

Woods, D. L., S. H. Ridgeway, D. G. Carter, and T. H. Bullock (1985) Middle- and long-latency auditory event-related potentials in dolphins. In *Dolphin Cognition and Behavior: A Comparative Approach,* R. J. Schusterman, J. A. Thomas, and F. G. Wood, eds., Erlbaum, Hillsdale, NJ.

Yingling, C. C., and Y. Hosobuchi (1984) A subcortical correlate of P300 in man. Electroencephalogr. Clin. Neurophysiol. *59:* 72–76.

Zhang, J. X., C. Wilson, M. Levesque, R. M. Harper, and J. Engel (1988) A multi-modal, multi-plane computer imaging system for stereotaxic neurosurgery. Soc. Neurosci. Abstr. *14:* 340.